Vacuum 100 (2014) 36–40

Contents lists available at ScienceDirect

Vacuum

journal homepage: www.elsevier.com/locate/vacuum

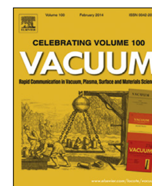

Rapid communication

Real-time stress evolution during early growth stages of sputter-deposited metal films: Influence of adatom mobility

G. Abadias*, A. Fillon, J.J. Colin, A. Michel, C. Jaouen

Institut P', Département Physique et Mécanique des Matériaux, Université de Poitiers – CNRS – ENSMA, SP2MI, Téléport 2, Bd M & P. Curie, F86962 Chasseneuil-Futuroscope cedex, France

A R T I C L E   I N F O

Article history:
Received 14 June 2013
Received in revised form
20 July 2013
Accepted 22 July 2013

Keywords:
Stress
Sputtering
Metallic films
Surface diffusivity
Interface stress
Coalescence
Nucleation and growth

A B S T R A C T

Using a multi-beam optical stress sensor, the real-time stress evolution during the early growth stages of a large class of sputter-deposited metal (Me) films is studied with monolayer sensitivity. For high-mobility fcc (Ag, Au, Pd) metals, a typical compressive–tensile–compressive (CTC) behavior is observed, characteristic of a Volmer-Weber growth mode. A correlation between the homologous temperature (T_s/T_m), tensile stress peak position, grain size and steady-state compressive stress in the post-coalescence stage is presented. For low-mobility bcc (Mo, W, Ta) metals ($T_s/T_m \leq 0.10$) deposited on *a*-Si, kinetic limitations result in a 2D growth mode highly influenced by interfacial effects. The film force is initially dominated by change in surface stress, which scales with the surface energy difference $\Delta\gamma = \gamma_{Me} - \gamma_{a\text{-}Si}$. For both Mo and W, a stress transient is observed in the 2–4 nm range, followed by the development of unexpectedly large tensile stress, ascribed to a phase transition towards their equilibrium α-Mo and α-W structure. Such transient is not evidenced during Ta growth for which a compressive stress regime is steadily established and related to the growth of its metastable β-Ta structure. For all low-mobility metals, the final stress regime is controlled by the energetics of the incoming species and intrinsic mechanical properties of the material.

© 2013 Elsevier Ltd. All rights reserved.

The understanding of the physical origins of stress development during growth of polycrystalline thin films has been the subject of intense investigations [1–4]. Metallic thin films grown by physical vapor deposition can usually bear stress levels up to several GPa, well in excess of their corresponding yield stress in bulk form. Such excessive stress can lead to premature failure, accompanied with buckling or delamination. Significant progress has been made in the last decade thanks to the potentiality offered by *in situ*, real-time stress measurement during deposition, enabling one to probe the growth dynamics with sub-monolayer sensitivity. Several quantitative models have been proposed to relate the growth-induced stresses to changes in film microstructure, surface morphology, as well as incorporation of defects or influence of adsorbed species [5–11]. Up to date, the case of low-mobility metals has attracted much less attention than the case of high-mobility metals, known to grow typically in the Volmer-Weber mode, and for which the experimental data could be successfully explained by the proposed models [4–9]. More specifically, most of the data obtained on refractory metallic films (e.g., Mo, Ta) deposited by sputtering dated back to the pioneering works of Hoffman and Thornton [12], and were not focused on the initial growth stages. Our recent study on sputtered Mo(Si) thin films has highlighted the prime role of interfaces in governing the stabilization of amorphous layers and subsequent phase-transformation induced tensile stress [13].

The aim of this paper is to provide a brief overview of the typical stress evolutions encountered during sputter-deposition of a large variety of metals, spanning both low- and high-adatom mobility conditions. In the present work, emphasis is laid on the careful examination of the early growth stages, using a real-time stress sensor combined with post-growth structural and morphological characterization. As illustrated on some typical examples, this approach provides valuable and unique information on the nucleation process and related mechanisms at the origin of stress development.

All films were grown at room temperature (RT) using dc balanced magnetron sputter-deposition in a high vacuum chamber (base pressure $\sim 5 \times 10^{-6}$ Pa) equipped with water-cooled, 3 inch-diameter high purity (>99.95%) metallic targets. The large target-

* Corresponding author. Tel.: +33 549496748.
E-mail address: gregory.abadias@univ-poitiers.fr (G. Abadias).

0042-207X/$ – see front matter © 2013 Elsevier Ltd. All rights reserved.
http://dx.doi.org/10.1016/j.vacuum.2013.07.041

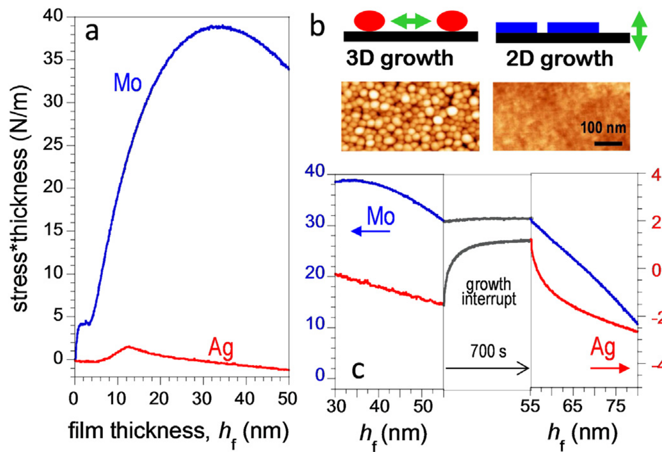

Fig. 1. (a) Comparative film force evolution during sputter deposition of Ag (R = 0.105 nm/s, P_{Ar} = 0.35 Pa) and Mo (R = 0.056 nm/s, P_{Ar} = 0.11 Pa) films on amorphous substrate. (b) 500 nm × 250 nm AFM surface topography images (z-scale:0–15 nm) of Ag (h_f = 3.1 nm) and Mo (h_f = 6.7 nm) films, and corresponding schematics of 3D (Ag) and 2D-like (Mo) growth mode. (c) Film force evolution before, during and after growth interrupt at $h_f \sim 55$ nm for both films. Note the different vertical scales: left (blue) for Mo and right (red) for Ag. (For interpretation of the references to color in this figure legend, the reader is referred to the web version of this article.)

to-substrate distance (18 cm) combined with the use of relatively low deposition flux (growth rate $R \leq 0.1$ nm/s) leads to minimize non intentional heating of substrate from plasma and sources, as the maximum temperature rise measured during growth of Mo film was ~10 °C. Deposition was carried at constant power using Ar plasma discharges on amorphous substrates: either native oxide (a-SiO_x) covered Si wafers or 9 nm thick amorphous Si sublayers (a-Si) sputter-deposited on Si wafers. The real-time stress evolution during growth was determined from the measurement of the substrate curvature change $\Delta\kappa$ using a multiple beam optical stress sensor (MOSS) designed by kSA, with a curvature sensitivity of 2×10^{-4} m^{-1}. More details on the experimental set-up can be found in Ref. [14]. Note that the curvature is proportional to the product $\sigma_{ave} \times h_f$ (also referred as the film force per unit width), where σ_{ave} is the average biaxial stress and h_f the film thickness. The crystal structure of the as-deposited films was determined using *ex situ* X-ray diffraction (XRD), while the surface morphology was observed, immediately after growth, using atomic force microscopy (AFM) operating at ambient air in tapping mode. The average grain diameter, L, was estimated from AFM images using a watershed algorithm in WSxM software, which consisted in detecting grain perimeter above a given height threshold, after careful planefit subtraction.

Fig. 1 shows comparatively the evolution of the film force per unit width of Mo and Ag films deposited on a-Si and a-SiO_x substrates, respectively. These two metallic films are representative of

Table 1
Physical and experimental quantities relevant to high-mobility metal films considered in the present study: homologous temperature T_s/T_m, surface energy γ_{111}, biaxial modulus M_{111}; deposition rate R, Ar working pressure P_{Ar}, critical thickness at film continuity h_{cont} and steady-state stress in final growth regime σ_{ss}. In all cases, the elastic modulus and surface energy are given for the dense {111} planes of the equilibrium fcc structure. The surface energy of the native a-SiO_x layer is ~1.0 J m^{-2}.

	T_s/T_m	γ_{111} (J m^{-2})	M_{111} (GPa)	R (nm/s)	P_{Ar} (Pa)	h_{cont} (nm)	σ_{ss} (GPa)
Ag	0.24	1.25	174	0.105	0.75	16.5	−0.05
Au	0.22	1.5	190	0.085	0.75	10.5	−0.22
Pd	0.16	2.0	288	0.076	0.16	6.0	−0.28

Table 2
Physical and experimental quantities relevant to low-mobility metal films considered in the present study: homologous temperature T_s/T_m, surface energy γ_{110}, biaxial modulus M_{110}; deposition rate R, Ar working pressure P_{Ar}, screening length ξ and steady-state stress in final growth regime σ_{ss}. In all cases, the elastic modulus and surface energy are given for the dense {110} planes of the equilibrium bcc structure. The surface energy of the a-Si sublayer is $\gamma_{a\text{-Si}} \sim 1.07$ J m^{-2}.

	T_s/T_m	γ_{110} (J m^{-2})	M_{110} (GPa)	R (nm/s)	P_{Ar} (Pa)	ξ (nm)	σ_{ss} (GPa)
Mo	0.10	2.91; 3.00	414	0.056	0.24	0.30 ± 0.05	−0.60*
Ta	0.09	2.90; 3.15	313	0.050	0.23	0.39 ± 0.02	−1.40
W	0.08	3.27; 3.68	571	0.049	0.20	0.56 ± 0.02	−2.25

* At R = 0.12 nm/s.

low- and high-adatom mobility conditions, respectively, if one refers to the homologous temperature T_s/T_m, where T_s is the substrate temperature during growth and T_m the melting temperature of the material (see Tables 1 and 2). Very distinct stress evolutions, both in sign and amplitude, are obvious. Sputter-deposited Ag films (T_s/T_m = 0.24) exhibit a characteristic CTC (compressive–tensile–compressive) stress behavior, associated with the different stages of Volmer-Weber growth mode, as confirmed by the formation of 3D islands (see AFM image of Fig. 1b). The three stages are better visualized in Fig. 2. The first compressive stage has been attributed to the nucleation and growth of isolated islands (referred as pre-

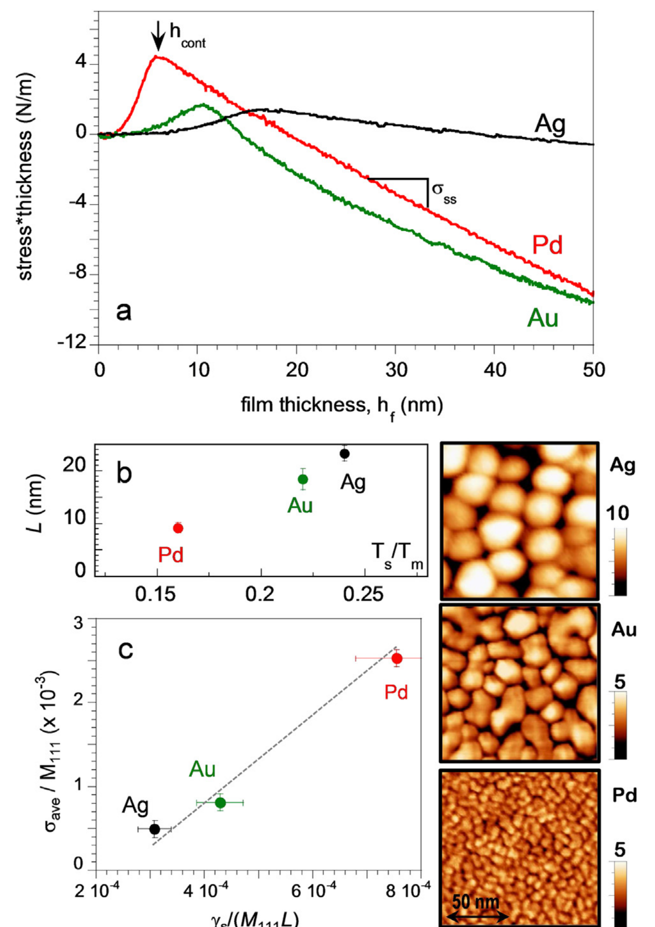

Fig. 2. (a) Film force evolution during sputter deposition of Ag, Au and Pd films on a-SiO_x. The film thickness corresponding to the tensile peak is referred as h_{cont}. (b) Evolution of average grain diameter, L, as derived from AFM surface topography images of Ag (h_f = 3.1 nm), Au (h_f = 3.4 nm) and Pd (h_f = 2.3 nm) films. (c) Evolution of σ_{ave}/M_{111} as a function of $\gamma_s/(M_{111}L)$ for Ag, Au and Pd films.

Download English Version:

https://daneshyari.com/en/article/1688412

Download Persian Version:

https://daneshyari.com/article/1688412

Daneshyari.com